00246

# EARTHQUAKE RESISTANT DESIGN OF HIGHWAY BRIDGES USING LAMINATED RUBBER BEARINGS: AN APPROACH FOR MODELING HYSTERETIC BEHAVIOR BASED ON EXPERIMENTAL CHARACTERIZATION OF RHEOLOGY PROPERTIES

A. R. Bhuiyan[1], Y. Okui[2], M.K. Razzak[2], A.F.M.S. Amin[3]


## ABSTRACT

The analytical steps for modeling the hysteretic behavior by utilizing experimental results on mechanical characteristics of full scale bearings under uni-directional horizontal displacement and a constant vertical compressive load are reported. An experimental scheme motivated from the early contribution of this Research Group on material level investigation and characterization of NR and HDR is introduced here to characterize the viscosity induced rate-dependent phenomena along with rate-independent elastic behavior of rubber bearings. Three types of bearings are used in this study: natural rubber bearing (RB), lead rubber bearing (LRB), and high damping rubber bearing (HDRB). In order to characterize the viscosity induced rate-dependent phenomena along with rate-independent elaso-plastic behavior of the bearings, an experimental scheme comprised of sinusoidal excitation (Basic) test, multi-step relaxation (MSR) tests, cyclic shear (CS) test, and simple relaxation (SR) tests is carried out. Presentation of the rate-dependent rheology model of the bearing devices follows thereafter. Finally, a set of parameters for three bearings are identified, which are subsequently used in simulating the mechanical behavior of the bearings as obtained using the basic test. The simulation results and comparison with independent experiments confirm the capability of the rheology model in predicting hysteretic response from RB, LRB, and HDRB.


## Introduction

Laminated rubber bearings have been considered to be an efficient technology for providing mitigation of seismic damage for structures and equipments and subsequently has proven to be reliable and cost effective (Abe et al. 2004a). Among the laminated rubber bearings, natural rubber bearing (RB) that uses natural rubber material has flexibility and small damping. On the other hand, the other two types of bearings, have high damping, and are widely used in many civil and architectural structures: one is the lead rubber bearing (LRB), which inserts a lead plug into the RB to provide hysteretic damping and the other is high damping rubber bearing (HDRB), which possesses high damping in order to provide energy absorbing property.

Several experimental works were conducted under uni-direction and bi-axial horizontal deformations with constant vertical loads in order to study the mechanical properties of the bearings (Abe et al., 2004a and Kikuchi and Aiken, 1997). Several types of bearings were used in

[1]Department of Civil Engineering, Chittagong University of Engineering & Technology, Chittagong, Bangladesh

[2] Department of Civil and Environmental Engineering, Saitama University, Saitama 338-8570, Japan

[3]Department of Civil Engineering, Bangladesh University of Engineering and Technology, Dhaka, Bangladesh

their studies. They have identified some aspects of bearings, such as hardening and dependence of the restoring forces on the maximum shear strain amplitude experienced in the past. Motivated by the experimental results of the bearings, different forms of analytical models for bearings are proposed by them (i.e. Abe et al., 2004b; Kikuchi and Aiken, 1997 etc.). However, their studies are mostly related to illustrating the strain-rate independent hysteretic behavior of the bearings. Furthermore, Dall'Asta and Ragni (2006) and Hwang et al. (2002) have studied the mechanical behavior of high damping rubber dissipating devices by conducting different experiments, such as sinusoidal loading tests at different frequencies, cyclic shear tests at different strain-rates along with relaxation tests. They have identified the strain-rate dependence of the restoring forces and subsequently developed rate-dependent analytical models. However, separation of the rate-dependent behavior from other mechanical behavior is not clearly addressed in their studies.

Furthermore, a number of experimental and numerical works on high damping rubber (HDR) materials have been performed in the past (Amin et al., 2002, 2006). These fundamental works show that the mechanical properties of HDR materials are dominated by the nonlinear rate-dependence including other inelastic behavior. Moreover, the different viscosity behavior in loading and unloading has been identified. Based on these propositions and subsequent characterizations proposed therein, the current study was aimed towards constructing analytical steps for modeling the rate-dependent hysteretic behavior by utilizing experimentally observed data on mechanical characteristics of full scale bearings under uni-directional horizontal displacement and a constant vertical compressive load. To this end, an experimental scheme comprised of sinusoidal excitation (Basic) test, multi-step relaxation (MSR) tests, cyclic shear (CS) test, and simple relaxation (SR) tests is carried out on three types of bearings: natural rubber bearing (RB), lead rubber bearing (LRB), and high damping bearing (HDRB). A rate-dependent rheology model of the bearings is presented thereafter. Finally, a set of parameters for three bearings are identified, which are subsequently used in simulating the mechanical behavior of the bearings as obtained using the basic test. The simulation results and comparison with independent experiments confirm the capability of the rheology model in predicting hysteretic response from RB, LRB, and HDRB

## Mechanical Behavior

### Specimens

All the specimens were square cross-sectional shape with external in-plane dimensions equal to 250 mm x 250 mm. The reinforcing steel plates had similarly a square planar geometry with external dimensions of 240 mm x 240 mm and thickness of 2.3 mm each. The dimensions and material properties of these specimens are given in Table 1. The dimensions of the test specimens were selected following the ISO standard (ISO, 2005).

Table 1. Geometry and material properties

| Specifications | Laminated rubber bearings | | |
|---|---|---|---|
| | HDR3 | LRB2 | RB1 |
| Cross-section (mm) | | 240X240 | |
| Number of rubber layers | | 6 | |
| Thickness of one rubber layer (mm) | | 5.0 | |
| Thickness of one steel layer (mm) | | 2.3 | |
| Diameter of lead plug (mm) | -- | 34.5 | -- |
| No. of lead plugs | -- | 4 | -- |
| Nominal shear modulus (MPa) | | 1.2 | |

**Experimental Set-up and Loading Conditions**

The specimens were tested in a computer-controlled servo-hydraulic testing machine at room temperature ($23^0$C). Displacement controlled tests, under shear deformation with an average constant vertical compressive stress of 6 MPa, were carried out. The displacement was applied along the top edge of the specimen and the force response was measured with two load cells. All data were recorded using a personal computer. Some of the experimental results are also discussed in somewhere else (Bhuiyan, 2009; Bhuiyan et al., 2009).

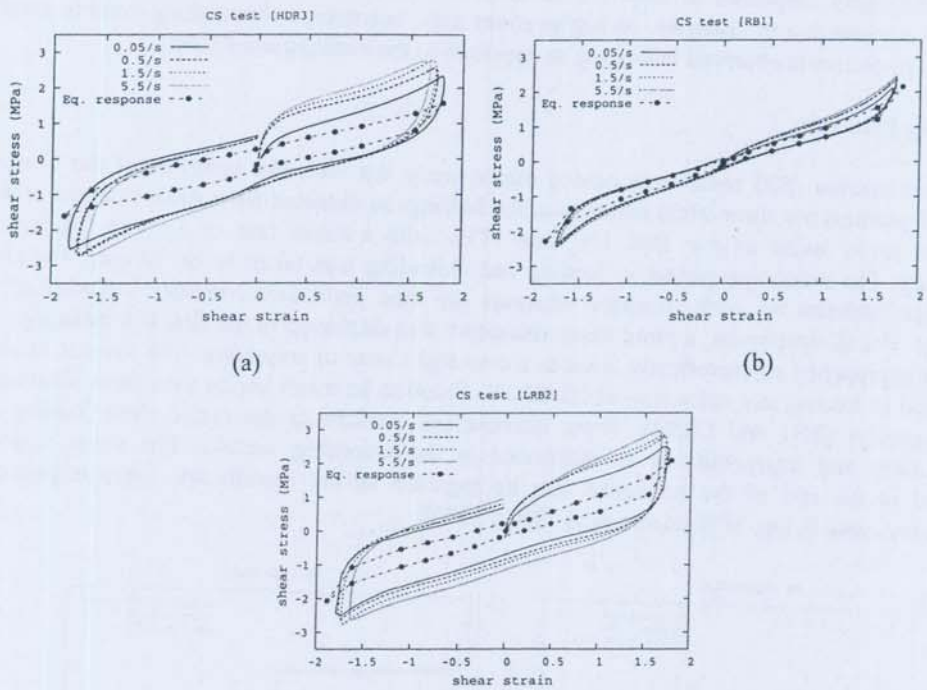


(a) (b)

(c)

Figure 1. Shear stress-strain relationships obtained from CS tests at different strain rates of the bearings; (a) HDR3, (b) RB1, (c) LRB; equilibrium response as obtained from MSR tests is also presented for clear comparison.

**Strain-Rate Dependent Behavior**

With a view to understanding the mechanical behavior of the bearings regarding the strain rate-dependence, a series of cyclic shear tests (CS tests) at different strain rates from 0.05/s to 5.5/s were carried out. Figs. 1(a), (b), and (c) show the strain-rate dependence of shear stress-strain responses in HDR3, RB1, and LRB2 bearings, respectively, observed in different strain-rates. The stress responses in the loading path contain a three-characteristic features like a high initial stiffness feature at low strain levels followed by a traceable large flexibility at moderate strain levels as well as a large strain-hardening feature at the end. When compared among the three bearings, the high initial stiffness at a low strain level and the high strain hardening at a high strain level are mostly prominent in HDR3 at a higher strain rates. However, a weaker strain-hardening feature in LRB2 than that of the other specimens at higher strain levels is also noticeable. A comparison of hysteresis loops observed at different strain rates shows that the size of the

 00249

hysteresis loops increases with increase of strain rates as shown in Figs.1 (a) to (c). While comparing among all the bearings, the HDR3 demonstrates a bigger hysteresis loop in compared with the other bearings (RB1 and LRB2).This typical behavior can be attributed that the HDR inherits relatively high viscosity property than that in other bearings. Another comparison of shear stress responses at different strain rates of the bearings shown in Figs. 1(a) to (c) indicates that the strong strain-rate dependence exists in loading, whereas much weaker strain-rate dependence is observed in unloading. The different viscosity property in loading and unloading is attributed to this typical experimental observation. A further comparison as shown in Figs. 1(a) to (c) between the loading-path responses at different strain-rates shows that with increasing strain-rate, the stresses increase due to viscosity. At higher strain rates, however, a diminishing trend in increase of stress responses is observed indicating an approach to the instantaneous state.

**Viscosity Behavior**

Simple relaxation (SR) tests were carried out to study the viscosity behavior of the bearings. Figure 2 presents the shear stress histories of the bearings as obtained from strain histories at three different strain levels of $\gamma$ = 100, 150, and 175% with a strain rate of 5.5/s in loading and unloading. The relaxation period in loading and unloading was taken to be 30 min. The stress relaxation histories on each specimen illustrate the time dependent viscosity behavior of the bearings. For all specimens, a rapid stress relaxation was displayed in the first few minutes; after while it approached asymptotically towards a converged state of responses. The amount of stress relaxation in loading and unloading of HDR3 was found to be much higher than those obtained in other bearings (RB1 and LRB2). These observations confirm to the cyclic shear loading test observations and interpretations as mentioned in the preceding section. The stress response obtained at the end of the relaxation can be regarded as the equilibrium stress response in asymptotic sense (Lion, 1996; Amin et al., 2002, 2006).

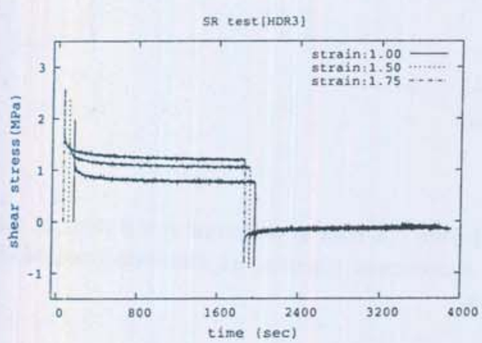


(a)

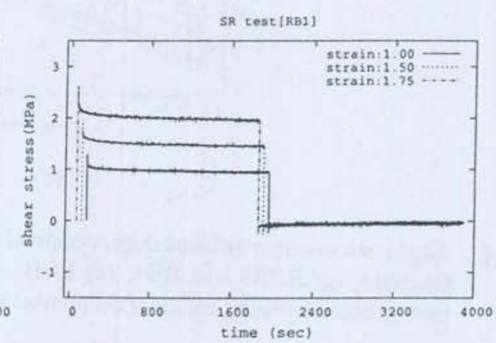


(b)

Figure 2. Shear stress histories obtained from SR tests of the bearings at different strain levels (a) HDR3, (b) RB1. Results for LRB2 are skipped for brevity. For clear illustration, the stress histories have been separated by 50 sec from each other.

**Static Equilibrium Hysteresis**

The experimental results obtained from the SR tests at different strain levels showed reduction in stress response during the hold time and approached the asymptotically converged state of responses (i.e equilibrium response). In this context, multi-step relaxation (MSR) tests were carried out to observe the relaxation behavior in loading and unloading paths and to obtain the equilibrium responses (e.g. time-independent response). Figure 3 illustrates the equilibrium responses of the bearing as obtained from the MSR tests. The equilibrium responses of the bearings were obtained by connecting the asymptotically converged stress values at each strain levels considered in the

MSR tests (Fig. 3).

00250

**Rheology Model and Parameter Identification**

Motivated by the experimentally revealed mechanical behavior of the bearings as presented in the preceding section a rate-dependent rheology model as shown in Fig. 4 is discussed as follows.

From the model structure shown in Fig. 4, the total stress and strain can be decomposed as:

$$\tau=\tau_{ep}+\tau_{ee}+\tau_{oe}\,;\ \ \gamma=\gamma_a+\gamma_s=\gamma_c+\gamma_d \tag{1}$$

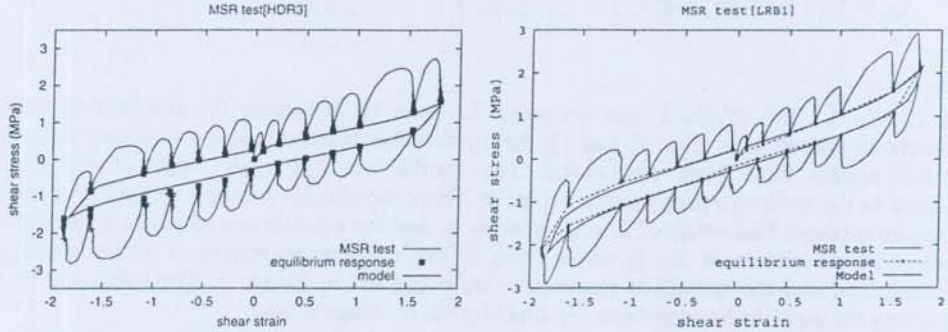


(a) (b)

Figure 3. Equilibrium stress responses of the bearings as obtained from MSR tests (a) HDR3, (b) LRB2. Results for RB1 are skipped for brevity.

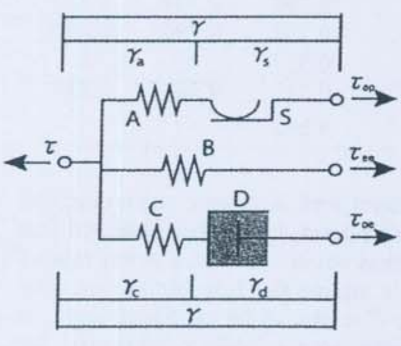


The rheology model is an extended version of the standard 3-paramer solid (Amin et al., 2002, 2006) by adding one slider with a spring in parallel to the original model. In the model, the first branch comprising of a spring (Element A) and a slider (Element S) represents the elasto-plastic response; the second branch of a spring (Element B) represents the nonlinear elastic response and these two branches together constitute the rate- independent response. On the other hand, the third branch consisting of a spring (Element C) and dashpot (Element D) represents the overstress resulting in the rate-dependent behavior.

Figure 4. Structure of the rheology model of the bearings

As seen in the MSR test results, this equilibrium hysteresis loop can be suitably represented by combining the ideal elasto-plastic response (First branch of the model, Figure 4) and the nonlinear elastic response. From equilibrium consideration, the stress on the spring is $\tau_{ep}$,(Element A) which the stress-strain relation can be expressed as

$$\tau_{ep}=C_1\gamma_a\,,\qquad \begin{cases}\dot{\gamma}_s\neq 0 & \left|\tau_{ep}\right|=\tau_{cr}\\ \dot{\gamma}_s=0 & \left|\tau_{ep}\right|<\tau_{cr}\end{cases} \tag{2}$$

 00251

where $C_1$ is a constant and $\gamma_a$ stands for the strain of the spring A. Element S is a friction slider. The mechanical response of the slider (Element S) is characterized by the condition that the friction slider is active only when the stress level in the slider reaches a critical shear stress $\tau_{cr}$ i.e. the stress $\tau_{ep}$ in the slider cannot be greater in absolute value than $\tau_{cr}$ which can be mathematically expressed as stated above.

The nonlinear elastic response as obtained from MSR test results with strain hardening at higher strain levels can be described by a non-Hookean nonlinear spring (Element B) (Figure 4)

$$\tau_{ee} = C_2\gamma + C_3|\gamma|^m \operatorname{sign}(\gamma), \qquad \operatorname{sgn}(x) = \begin{cases} +1 & : \; x > 0 \\ 0 & : \; x = 0 \\ -1 & : \; x < 0 \end{cases} \tag{3}$$

where $C_2$, $C_3$, $C_4$ and m (m>1) are constants. In order to determine the equilibrium response parameters as presented in Eqs. (2 and 3), the equilibrium hysteresis loops as obtained from the MSR test results have been considered. The equilibrium hysteresis loops of the bearings considered in the study are presented in Figure 3. These parameters are determined using standard least square method. The obtained critical stresses $\tau_{cr}$ and the equilibrium response parameters $C_2$, $C_3$, and $m$ for all specimens are given in Table 2. The equilibrium responses obtained using the proposed model and the identified parameters are presented in Figure 3. The solid line in each figure shows the equilibrium responses obtained by the rheology model.

Table 2. Rate-independent parameters

| Parameters | Laminated rubber bearings | | |
|---|---|---|---|
| | HDR | LRB | RB |
| $C_1$ (MPa) | 2.101 | 4.181 | 1.952 |
| $C_2$ (MPa) | 0.595 | 0.779 | 0.798 |
| $C_3$ (MPa) | 0.002 | 0.011 | 0.005 |
| $C_4$ (MPa) | 2.653 | 2.351 | 0.401 |
| $\tau_{cr}$ (MPa) | 0.296 | 0.231 | 0.130 |
| m | 7.423 | 6.681 | 7.853 |

Table 3. Rate-dependent parameters

| Parameters | Laminated rubber bearings | | |
|---|---|---|---|
| | HDR | LRB | RB |
| $A_l$ (MPa) | 0.752 | 0.794 | 0.553 |
| $A_u$ (MPa) | 0.751 | 0.794 | 0.553 |
| q | 0.352 | 0 | 0 |
| n | 0.211 | 0.302 | 0.232 |
| $\xi$ | 1.242 | - | - |

From the CS test results, a diminishing trend of the stress responses with increasing strain rates can be observed in all bearings as illustrated in Figure 1. From these figures, it has been observed that the instantaneous response lies at the neighborhood of the stress-strain curve at a strain rate of 5.5/s for the HDR3 and the LRB2; however for the RB1, it is around the 1.5/s strain rate. The instantaneous stress-strain curve, and accordingly the spring C seems to be nonlinear even in loading regime as visualized in the figure. For simplicity, a linear spring model is employed for Element C in order to reproduce the instantaneous response of the bearings:

$$\tau_{oe} = C_4\gamma_c, \tag{4}$$

where $C_4$ is the spring constant for Element C. The parameter $C_4$ is determined so that the instantaneous stress-strain curve calculated from the rheology model ($\tau = \tau_{ee} + \tau_{ep} + \tau_{oe}$ (without the dashpot element)) can envelop the stress-strain curves obtained from the CS test. The obtained parameters $C_4$ for all bearings are listed in Table 2.

From the stress relaxation results of the MSR and the SR loading tests, the time histories of the total stress $\tau$ and the total strain $\gamma$ are obtained. Assuming that the asymptotic stress response at the end of each relaxation period is the equilibrium stress $\tau_{eq}$ at a particular strain level, the overstress history $\tau_{oe}$ in each relaxation period can be obtained by subtracting the equilibrium stress from the total stress. Using Eqs. (3) and (4) and a moving averaging technique over the experimental data (Bhuiyan, 2009) yield the overstress and dashpot strain rates for Element D. The overstress-dashpot strain rate relations for the bearings is expressed (Bhuiyan et al., 2009) by



$$\tau_{oe} = A\left|\frac{\dot{\gamma}_d}{\dot{\gamma}_o}\right|^n \operatorname{sgn}(\dot{\gamma}_d), \quad A = \frac{1}{2}\left(A_l \exp(q|\dot{\gamma}|) + A_u\right) + \frac{1}{2}\left(A_l \exp(q|\dot{\gamma}|) - A_u\right)\tanh(\xi \tau_{oe} \dot{\gamma}_d) \qquad (5)$$

where $\dot{\gamma}_o = 1$ ($sec^{-1}$) is a reference strain rate of the dashpot; $A_l$, $A_u$, $q$ and $n$ are constants for nonlinear viscosity and $\xi$ is the smoothing parameter to switch viscosity between loading and unloading.

A standard method of nonlinear regression analysis is employed in Eq.5 to identify viscosity constants and smoothing parameter. SR/MSR test results were used for identifying the viscosity constants whereas, a sinusoidal excitation results were used for smoothing parameters. The identified parameters are given in Table 3.

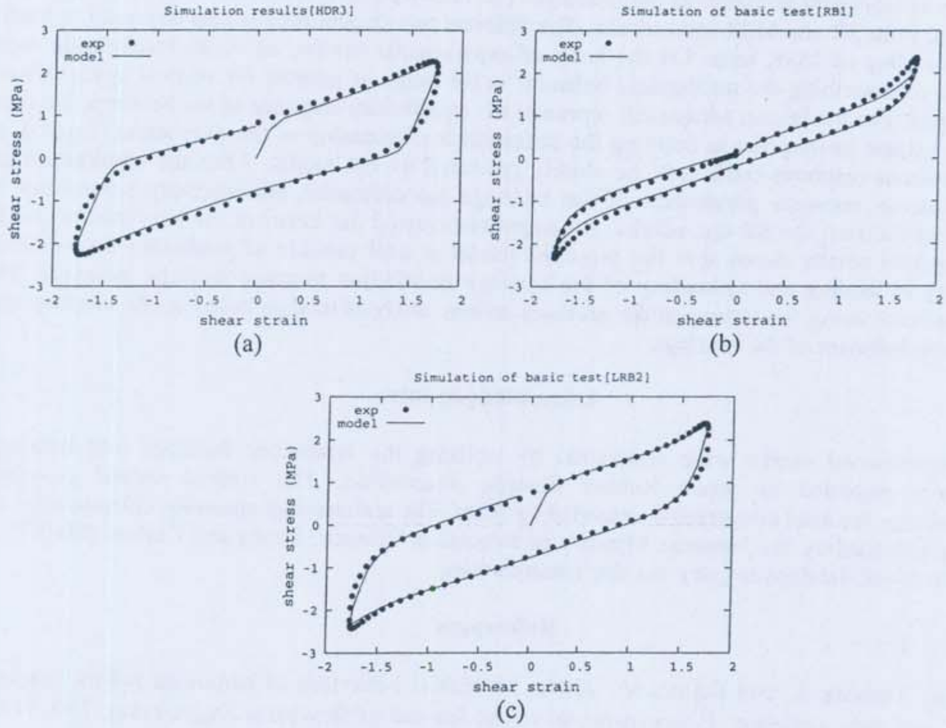


Figure 5. Numerical simulations of sinusoidal loading data of the bearings(a) HDR3, (b) RB1, (c) LRB2; the 4th cycle stress responses are considered in the simulations to simply remove the softening effect from the other inelastic behavior of the bearings.

## Numerical Simulations and Discussion

The experimental results presented in the preceding sections revealed the viscosity induced rate-dependent behavior along with other inelastic properties of three bearings (HDR3, RB1, and LRB2). Analytical steps for constructing a rate-dependent rheology model of the bearings utilizing the experimental results are discussed thereafter. In this Section, the proposed rheology model is used to simulate the experimental results obtained using the sinusoidal loading data. In order to remove the softening effect of the bearings, the 4th cycle shear stress-strain responses are used in the simulation. It is reported (Bhuiyan, 2009) that rate-independent responses of the bearings do not depend on the specimens' condition, i.e. whether it is virgin or preloading specimen. However, this dose not hold true for the rate-dependent responses of the bearings (Bhuiyan, 2009). Considering these facts, the parameters as shown in Table 2 along with a modified set viscosity parameters have been used for simulating the stress-strain responses obtained from sinusoidal excitation test (basic test). Figure 5 present the simulated stress responses of sinusoidal loading experiments for the three bearings. The results are comparable very closely with the experiments in predicting the stress responses in loading and unloading.

## Concluding Remarks

An experimental scheme was performed in order to investigate the mechanical behavior of three types of bearings under horizontal cyclic shear deformation with a constant vertical compressive load. The equilibrium response of the bearings can be asymptotically identified from MSR test results. The neighborhood of the instantaneous response of the bearings can be approximated by conducting a series of CS tests at different strain rates. These two experimental results represent the rate-independent response of the bearings. The rate-dependent behavior of the bearings can be obtained from SR and MSR tests results. The different rate-dependence is also observed in loading and unloading of MSR tests. On the basis of experimental results, an elasto-viscoplastic model capable of describing the mechanical behavior in the range of interest for seismic applications is developed. The model can adequately represent the equilibrium response of the bearings, however, due to a linear assumption in deriving the stress-strain relationship of the over stress (Eq.(5)), the instantaneous response could not be closely predicted by the model. After the equilibrium and instantaneous response parameters of the bearings are estimated, the viscosity parameters are identified utilizing the SR test results. A comparison carried out between the simulations and the experimental results shows that the proposed model is well capable of predicting the nonlinear viscosity in loading and unloading of the bearings in addition to other inelastic behavior. This permits overcoming limitations of the previous seismic analysis models based on the elasto-plastic hysteresis behavior of the bearings.

## Acknowledgements

The experimental works were conducted by utilizing the laboratory facilities and bearings-specimens provided by Japan Rubber Bearing Association. The authors indeed gratefully acknowledge the kind cooperation extended by them. The authors also sincerely acknowledge the funding provided by the Japanese Ministry of Education, Science, Sports and Culture (MEXT) in the form of scholarships to carry out this research work

## References

Abe, M., Yoshida, J., and Fujino, Y., 2004a. Multiaxial behaviors of laminated rubber bearings and their modeling. I: Experimental study, *Journal of Structural Engineering*, 130, 1119-1132.

Abe, M., Yoshida, J., and Fujino, Y., 2004b. Multiaxial behaviors of laminated rubber bearings and their modeling. II: Modeling, *Journal of Structural Engineering*, 130, 1133-1144.

Amin, A.F.M.S., Alam, M.S., Okui, Y., 2002. An improved hyperelasticity relation in modelling viscoelasticity response of natural and high damping rubbers in compression: experiments, parameter identification and numerical verification, *Mechanics of Materials*, 34, 75-95.

Amin, A.F.M.S., Lion, A., Sekita, S., Okui, Y., 2006. Nonlinear dependence of viscosity in modeling the rate-dependent response of natural and high damping rubbers in compression and shear: Experimental identification and numerical verification, *International Journal of Plasticity*, 22, 1610-1657.

Bhuiyan, A.R., 2009. *Rheology modeling of laminated rubber bearings for seismic analysis*, PhD Dissertation, Graduate School of Science and Engineering, Saitama University, Japan.

Bhuiyan, A.R., Okui, Y., Mitamura, H. and Imai, T., 2009. A rheology model of high damping rubber bearings for seismic analysis: identification of nonlinear viscosity, *International Journal of Solids and Structures*, 46, 1778-1792.

Dall'Asta, A., and Ragni, L., 2006. Experimental tests and analytical model of high damping rubber dissipating devices, *Engineering Structures,* 28, 1874-1884.

Hwang, J.S., Wu, J. D., Pan, T, C., and Yang, G., 2002. A mathematical hysteretic model for elastomeric isolation bearings, *Earthquake Engineering and Structural Dynamics,* 31, 771-789.

International Organization of Standardization (ISO), 2005. *Elastomeric seismic-protection isolators, Part 1: Test methods*, Geneva, Switzerland.

Kikuchi, M., and Aiken, I.D., 1997. An analytical hysteresis model for elastomeric seismic isolation bearings, *Earthquake Engineering and Structural Dynamics,* 26, 215-231.

Lion, A., 1996. A constitutive model for carbon black filled rubber: Experimental investigations and mathematical representation, *Continuum Mechanics and Thermodynamics*, 8, 153-169.